Behavioral/Systems/Cognitive

Animal-to-Animal Variability in Motor Pattern Production in Adults and during Growth

Dirk Bucher, Astrid A. Prinz, and Eve Marder
Volen Center and Biology Department, Brandeis University, Waltham, Massachusetts 02454-9110

Which features of network output are well preserved during growth of the nervous system and across different preparations of the same size? To address this issue, we characterized the pyloric rhythms generated by the stomatogastric nervous systems of 99 adult and 12 juvenile lobsters (*Homarus americanus*). Anatomical studies of single pyloric network neurons and of the whole stomatogastric ganglion (STG) showed that the STG and its neurons grow considerably from juvenile to adult. Despite these changes in size, intracellularly recorded membrane potential waveforms of pyloric network neurons and the phase relationships in the pyloric rhythm were very similar between juvenile and adult preparations. Across adult preparations, the cycle period and number of spikes per burst were not tightly maintained, but the mean phase relationships were independent of the period of the rhythm and relatively tightly maintained across preparations. We interpret this as evidence for homeostatic regulation of network activity.

Key words: **lobster; *Homarus americanus*; stomatogastric ganglion; central pattern generator; pyloric rhythm; homeostasis**

Introduction

How similar from animal to animal are the networks that control a specific behavior? We know anecdotally that animal performance in both simple behaviors and complex cognitive tasks varies among individuals, but there are relatively few attempts to assess the degree of variance in network outputs in preparations in which it is possible to both characterize the network and to understand the cellular mechanisms that give rise to those outputs. This question is particularly interesting in the light of recent experimental and theoretical studies of homeostasis of cellular and synaptic properties in the nervous system (Stemmler and Koch, 1999; Turrigiano, 1999; Marder and Prinz, 2002; Turrigiano and Nelson, 2004). These studies suggest that the intrinsic excitability of single neurons and synaptic strengths are subject to slow homeostatic regulation that can stabilize neuronal function despite ongoing turnover of channels and receptors (LeMasson et al., 1993; Turrigiano et al., 1995; Davis and Goodman, 1998; Liu et al., 1998; Desai et al., 1999; Golowasch et al., 1999a,b; Davis and Bezprozvanny, 2001; Aizenman et al., 2003; MacLean et al., 2003; Zhang and Linden, 2003). However, what really matters for the animal is not what the properties of single neurons are or how strong single synapses may be, but how the network performs. Therefore, it becomes critical to know exactly how tightly controlled network output is, both across animals and within an individual animal's lifetime.

Growth provides an interesting window into the regulation of network function. Of particular interest are networks that must function throughout the lifetime of the animal, while both the nervous system and the animal itself are growing. Does this mean that the changes in size of neurons, length of axons, and the number and density of channels and receptors are appropriately matched so that network function is maintained, or does network function change as the animal is growing?

In this paper, we take advantage of the well defined and relatively easy to characterize pyloric rhythm of the lobster stomatogastric ganglion (STG) (Harris-Warrick et al., 1992). We characterize the motor patterns across 99 individual STG preparations from adult *Homarus americanus* and from 12 preparations of juvenile animals. Because lobsters reach their adult form after metamorphosis when they are <1 inch long (Factor, 1995) and grow extensively after that time, they are ideally suited for asking how tightly network performance is maintained despite considerable changes in neuron and ganglion size and structure. The data in this paper establish the ranges of network outputs seen both as a consequence of growth and across individual animals, establishing benchmarks for determining which features of network function are tightly controlled and which are more variable in the population and during growth.

Materials and Methods

Adult lobsters (thorax length ≈84 mm), *Homarus americanus*, were purchased from Yankee Lobster (Boston, MA), and juvenile lobsters (thorax length 11.7–20.4 mm) were obtained from the Lobster Rearing and Research Facility at the New England Aquarium. Animals were kept at 10–13°C in recirculating artificial seawater tanks. All animals were cold-anesthetized before dissection. Dissections were performed in saline containing (in mM): 479.12 NaCl, 12.74 KCl, 13.67 $CaCl_2$, 20 Mg_2SO_4, 3.91 Na_2SO_4, and 5 HEPES, pH 7.4–7.5. The stomatogastric nervous system was dissected and pinned out in transparent Sylgard-coated (Dow Corning, Midland, MI) dishes containing chilled (9–13°C) saline. The paired commissural ganglia, the esophageal ganglion, STG, their connecting

Received Sept. 6, 2004; revised Nov. 29, 2004; accepted Dec. 21, 2004.

This work was supported by National Institutes of Health Grants S10 RR16780 and MH 46742 (E.M.), the Sloan–Swartz Center at Brandeis University, and Stipend BU 1361/1-1 of the Deutsche Forschungsgemeinschaft (D.B.). We thank V. Thirumalai, K. J. Rehm, S. R. Pulver, and A. L. Taylor for additional control data sets.

Correspondence should be addressed to Dr. Dirk Bucher, Volen Center, Brandeis University, MS 013, 415 South Street, Waltham, MA 02454-9110. E-mail: bucher@brandeis.edu.

DOI:10.1523/JNEUROSCI.3679-04.2005

 0270-6474/05/251611-09$15.00/0

nerves, and the main peripheral motor nerves were kept intact. The STG was always desheathed.

Electrophysiological recordings. The pyloric rhythm was characterized using the activity of a selected group of neurons that are active in a triphasic pattern. The two pyloric dilator (PD) neurons are motor neurons that are electrically coupled to a single interneuron, the anterior burster (AB) neuron. The PD and AB neurons make inhibitory connections onto the lateral pyloric (LP) neuron and the pyloric (PY) neurons. The PD neurons receive feedback from the follower neurons only through an inhibitory synapse from the LP neuron. The LP and PY neurons have reciprocal inhibitory connections.

Extracellular recordings were made with stainless steel wires from small (~1 mm) petroleum jelly wells around specific nerves. Extracellular spikes were recorded from the following neurons and in the following nerves (nomenclature after Maynard and Dando, 1974). The PD neurons were recorded from the pyloric dilator nerve (pdn). The LP neuron was either recorded from the ventral lateral ventricular nerve or the proximal part of the pyloric nerve (pyn). The amplitude of extracellular LP spikes is larger than that of other spikes in both nerves. The PY neurons were recorded from the distal part of the pyn. Spike detection was unambiguous for the PD and LP neurons. It is not known how many PY neurons exist in *Homarus americanus*. For comparison, there are five in *Cancer borealis* (Kilman and Marder, 1996) and eight in *Panulirus interruptus* (Selverston and Moulins, 1985). Summation of spikes prevents identification of individual PY neuron units in extracellular recordings. Therefore, no attempt was made to count spikes of the PY neurons. Analysis of PY neuron activity was restricted to identifying burst starts and ends.

Signals were amplified and filtered using a differential AC amplifier (A-M Systems, Carlsborg, WA). Intracellular recordings from the STG motor neuron somata were made using 30–50 MΩ glass microelectrodes filled with 0.6 M K_2SO_4 and 20 mM KCl and amplified using an Axoclamp 2B amplifier (Axon Instruments, Foster City, CA). Cells were identified by their characteristic waveforms and correspondence of intracellular spikes with extracellular spikes in the nerve recordings.

Data acquisition and analysis. Recordings were digitized using a Digi-Data 1200 data acquisition board (Axon Instruments) and analyzed in Spike2 (version 5; CED, Cambridge, UK) using programs written in the Spike2 script language. Statistical tests were performed in Statview (version 5; SAS Institute, Cary, NC) and programs written in C++ for both mean and cycle-to-cycle burst and phase parameters. Values are given as means ± SD, unless otherwise stated.

Dye filling and confocal microscopy. Neuronal morphology was revealed by iontophoretic injection of Alexa 568 hydrazide (Molecular Probes, Eugene, OR) into the soma. Ganglia were subsequently lifted off the cushion of connective tissue that is contiguous with the perineural sheath of the nerves (Maynard and Dando, 1974). The connective tissue underneath the cell body region was removed. The two nerves connecting the STG to the rest of the nervous system (stomatogastric nerve and dorsal ventricular nerve) were cut several millimeters away from the ganglion and the cut ends pinned to the Sylgard. The closest paired side nerves above (anterior ventricular nerve) and below (anterior gastric nerve) the ganglion were also pinned for stability. The ganglia were then fixed in 4% paraformaldehyde (Electron Microscopy Sciences, Hatfield, PA) for 20 min, rinsed in 0.1 M phosphate buffer, dehydrated in an ethanol series (30, 50, 70, 90, 100%, 5 min each), and mounted in methyl salicylate. Confocal imaging was performed using a Leica TCS confocal microscope. The autofluorescence of the tissue was scanned for measurements of ganglion dimensions, and care was taken to avoid scaling artifacts caused by tissue shrinking and refractive index mismatch (Bucher et al., 2000). Image processing and analysis were done using AMIRA software (version 3.0; TGS, San Diego, CA).

Results

Growth of the stomatogastric nervous system from juvenile to adult

After the final larval molt, lobsters (*Homarus americanus*) are "morphologically adult" but continue to grow throughout their lifetime. In the first 5–7 years they grow ~20-fold in length (Factor, 1995). Figure 1*A* illustrates the size difference between the immature juvenile animals (thorax length 11.7–20.4 mm; size range of the animals used in this study) and the mature adults. The large increase in body size means that sensory encoding of information and motor output must be adjusted to changes in physical dimensions while the nervous system itself is growing. The STG also grows substantially from juveniles to adults, albeit less so than the whole animal, as can be seen in the volume renderings of autofluorescence scans of a juvenile and an adult STG (Fig. 1*B*). Figure 1*C* shows surface reconstructions of the same ganglia, rendered from segmented image stacks that were used for the size measurements shown in Figure 1*D*. In *H. americanus*, the STG is spindle-shaped, and the neuronal cell bodies sit on the dorsal surface of the neuropil. All measurements were taken from the region between the anterior-most and posterior-most cell bodies. Length, width, depth, surface area, and volume were all significantly larger in adults than in juveniles ($p < 0.01$, unpaired *t* tests). Note that the STG does not grow isometrically, but instead changes shape during growth. Adult ganglia were 2.3 times longer than juveniles, but only 1.4 times wider and deeper, so

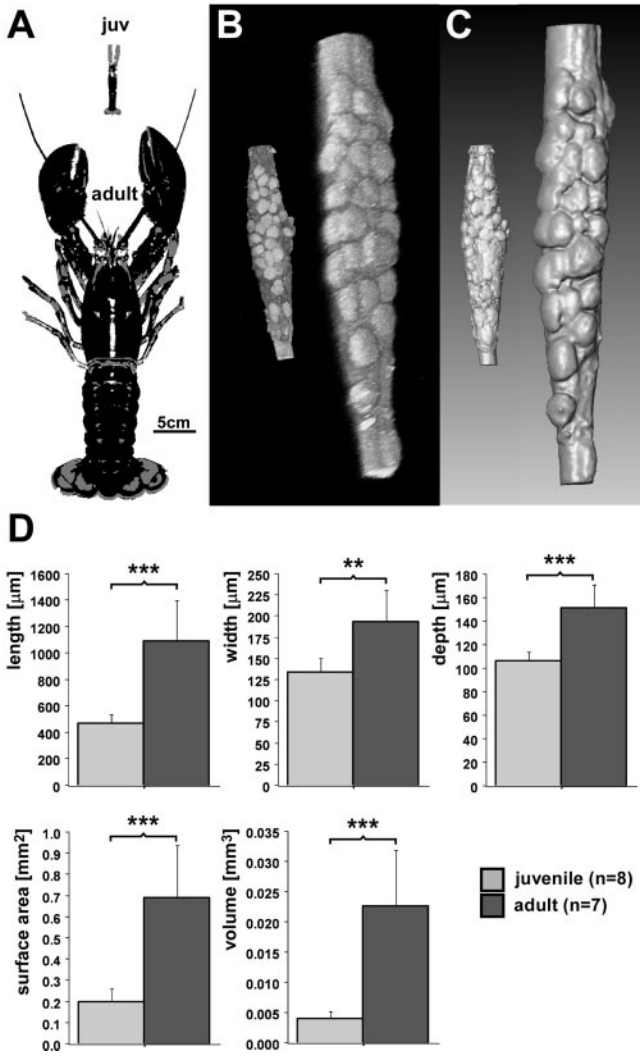

Figure 1. Growth of the stomatogastric ganglion in the lobster, *H. americanus*. *A*, Posterized photograph of a juvenile and an adult animal, representing the sizes used for this study. *B*, Volume rendering from confocal scans of the autofluorescence of a juvenile and an adult STG. *C*, Surface reconstructions of the same ganglia. *D*, Morphometric values obtained from segmented images of juvenile and adult STGs. All values were significantly larger in adults (unpaired *t* tests).

adult ganglia had a more elongated appearance. Surface area was 3.5 times larger, and volume 5.7 times larger in adults.

Growth potentially poses a challenge for neurons and the networks they form. The branching pattern and the length/diameter relationships in dendritic and axonal trees determine how signals propagate throughout the cell (Segev et al., 1995). During growth, the increased neuronal surface area will affect signal propagation unless the morphology and/or the channel densities are regulated accordingly (Hochner and Spira, 1987; Hill et al., 1994; Olsen et al., 1996). We filled a PD neuron in four juvenile and four adult preparations. The gross morphology of identified invertebrate neurons is often very constant from animal to animal, caused by stereotyped projection patterns through specific tracts and into specific neuropilar integration areas (Rowell, 1989). In contrast, the gross morphology of the PD neurons showed considerable variability even between individuals of the same age. Figure 2 shows maximum intensity projections of PD neuron fills in two juvenile and two adult STGs at the same scale. In both juveniles and adults the PD neurons have a very complex branching pattern. The diameters of soma, lower order branches, and axon approximately double from juvenile to adult. Although there appeared to be some characteristic branching "motifs," unambiguous identification of individual branches was not possible.

Growth could potentially alter the passive and active properties of a neuron. We therefore wanted to see whether the waveforms of membrane potential oscillations of pyloric neurons change during growth. Figure 3 shows simultaneous intracellular recordings from the cell bodies of PD, LP, and PY neurons from a juvenile and an adult STG. The overall membrane potential waveforms were similar in both stages. We used intracellular PD recordings to quantify burst and spike amplitudes in 10 juvenile and 10 adult animals. Only recordings were used in which the trough membrane potentials were −55 mV or lower, and firing patterns were not noticeably changed because of impalement. For the measurements of burst amplitudes, traces were low-pass filtered to remove spikes, and amplitudes were measured from trough to peak of the slow-wave membrane potential oscillation. The mean amplitude was 24.4 ± 4.7 mV in juveniles and 22.0 ± 7.0 mV in adults. These results were not significantly different (unpaired *t* test; $p = 0.365$). The somata of STG neurons do not produce regenerative activity, and fast membrane potential changes such as spikes are particularly subject to the low-pass filtering that the membrane capacitance imposes on electrical signals (Golowasch and Marder, 1992). Therefore, possible changes of the electrotonic structure during growth should most readily be detectable in the spike amplitudes recorded in the soma. Spike amplitudes were measured from averages triggered from the peak depolarizations of PD neurons. The mean amplitude was 8.9 ± 3.3 mV in juveniles and 9.1 ± 2.3 mV in adults. These results were not significantly different (unpaired *t* test; $p = 0.904$).

Motor neuron activity that is generated in the CNS is transmitted to muscle targets as action potentials that travel down the motor axons. During growth, peripheral nerves and motor neuron axons elongate, and alterations of action potential conduction times between the ganglion and periphery could change the relative timing of muscle activation and movement-related sensory feedback. The schematic in Figure 4*A* shows the increase in length of the major motor nerves to the pyloric muscles. The distance between the STG and the distal nerve recording sites increased from 13.3 ± 1.7 mm in juveniles ($n = 10$) to 48.6 ± 3.9 mm in adults ($n = 7$) ($p < 0.001$; unpaired *t* test). Figure 4*B* shows averaged traces of simultaneous recordings from the PD neuron soma and the pdn, triggered from the intracellular spike in a juvenile and an adult preparation. The conduction delay between STG and peripheral nerve recording sites increased significantly for all cell types ($p < 0.001$; unpaired *t* tests) (Fig. 4*C*), including the two lateral posterior gastric (LPG) neurons, which take part in both the pyloric and gastric rhythm and were analyzed here because their action potentials are also present in extracellular pyn recordings. Figure 4*D* shows that the conduction velocities (nerve distance/delay) changed relatively less, although they increased significantly for the PD ($p < 0.001$; unpaired *t* test) and the PY ($p < 0.01$; unpaired *t* test) axons. These changes in delay times are in the range of tens of milliseconds, whereas the

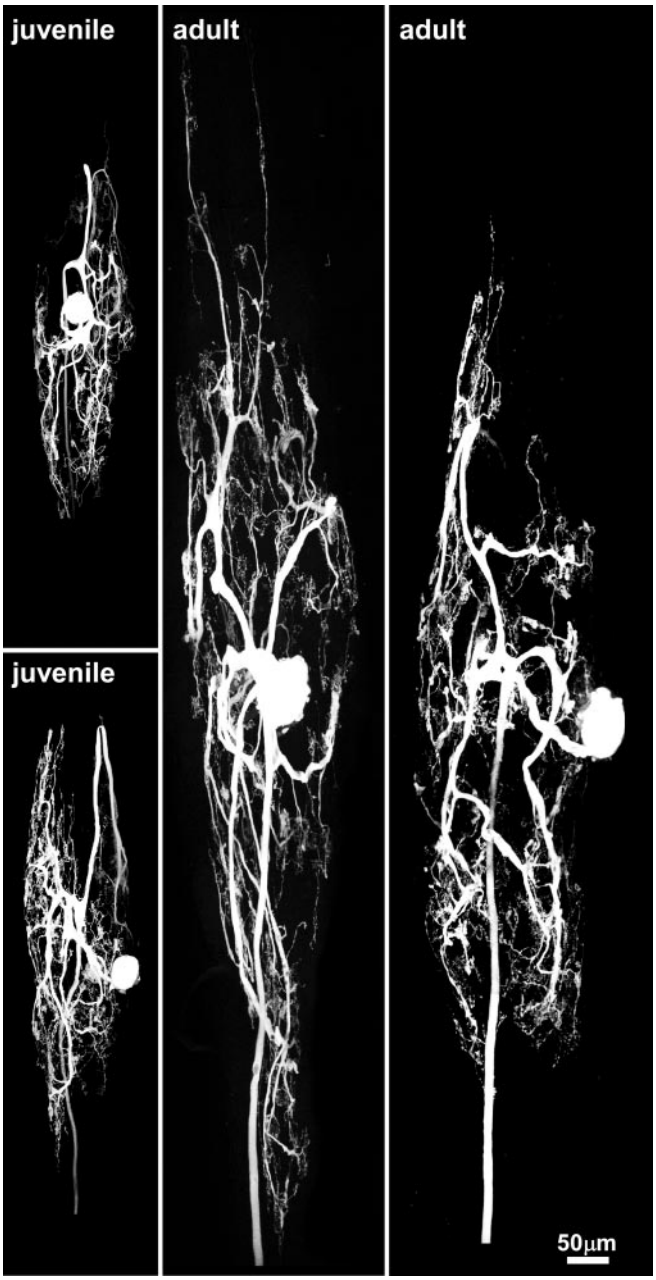

Figure 2. Growth of the stomatogastric ganglion. Maximum intensity projections of confocal images obtained from PD neurons filled with Alexa 568 hydrazide in two juvenile and two adult STGs. All projections are shown at the same scale (see scale bar in bottom right corner). Note the variability of gross morphological features.

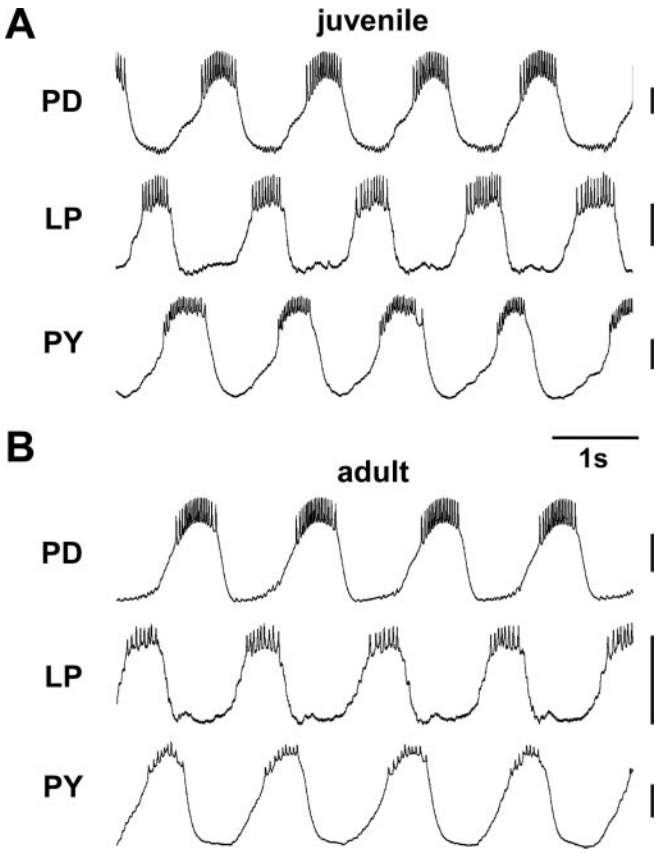

Figure 3. Simultaneous intracellular soma recordings of PD, LP, and PY in the juvenile and the adult. Calibration: 10 mV, 1 s. The cell body membrane of STG neurons does not produce regenerative activity, and spikes are therefore considerably attenuated in soma recordings.

pyloric cycle period is in the range of seconds. Thus, these changes in absolute timing of muscle activation and sensory feedback would be only a few percent of the period of the pyloric rhythm.

How similar is the pyloric rhythm from one animal to another?

Pyloric network output is characterized by some features that are qualitatively the same in every animal and, as shown above, are maintained throughout postlarval growth. Figure 5, *A* and *B*, shows two examples of extracellular nerve recordings of the pyloric rhythm in adult preparations, one with a relatively long cycle period, and one with a relatively short cycle period. The PD, LP, and PY neurons burst in a triphasic pattern in the same sequence. However, the cycle periods, the burst durations, and the latencies between bursts are different. We wanted to establish how much variability is found between preparations in the parameters that define the pyloric rhythm and can be quantified from extracellular recordings. The measurements we used for quantification are illustrated in Figure 5, *A* and *B*. Analysis was performed cycle-by-cycle for cycle periods and for the latencies of burst starts ("on") and burst ends ("off") with respect to the cycle start. We used PD bursts as the reference and measured cycle period from the start of one PD burst to the start of the next burst. Latencies were measured from the PD burst start to the PD burst end and from PD burst start to the burst starts and burst ends of LP and PY. We analyzed 2–20 min of pyloric nerve recordings (51–964 cycles per preparation) from 99 adult animals in this manner.

The histogram at the top of the plot in Figure 5*D* shows the distribution of mean cycle periods. Cycle periods were quite variable and not normally distributed around the mean, ranging from 1.10 to 2.50 s (mean: 1.52 ± 0.27). The mean values for PD off, LP on, LP off, PY on, and PY off are plotted against the mean cycle period for every preparation in Figure 5*C*. Regression analysis showed that all five mean latency values increased with mean cycle periods ($p < 0.001$ for each). They did so in a linear manner, because the R^2 values (the fractions of the variance of the latencies that are explained by the variance in cycle period) are high (PD on: 0.63; LP on: 0.70; LP off: 0.84; PY on: 0.81; PY off: 0.97). Furthermore, the latencies increased proportionally with the cycle period, because the *y* intercepts were not significantly different from zero (*p* values between 0.12 and 0.77). Proportional increase of latency with period means that the phase (latency normalized to the cycle period) does not change as a function of cycle period. Figure 5*D* shows phase plotted against the cycle period. The phases did not change significantly (*p* values between 0.07 and 0.78). Furthermore, the phase values were confined to a narrow range around the means, as can be seen from the histograms on the right of the plot. These data show that the cycle period was variable across preparations but that the values of phase relationships were well conserved from animal to animal.

Are phase relationships stable during growth?

Assuming that the consistency of the phase relationships of the pyloric motor pattern observed across adult preparations is the result of regulation of network activity, we wanted to know whether the same parameters are maintained during growth of the animal from juvenile to adult. We therefore analyzed the phase relationships in 12 juvenile animals.

Figure 6*A* shows an example extracellular recording from a juvenile. Because of the diminutive size of the peripheral nerves, LP and PY neuron spikes were always recorded from the entire pyn and discriminated by their shapes and amplitudes using spike shape template sorting and window discrimination in the Spike2 software. The pyloric rhythm cycle period in juveniles ranged from 1.34 to1.82 s (mean: 1.50 ± 0.15) and was not significantly different from adult cycle period (1.52 ± 0.27; $p = 0.87$) (Fig. 6*B*). Figure 6*C* shows the mean phase relationships in juveniles and adults. Phase relationships were similar in both, but LP on and LP off phase, as well as PY on phase were statistically different. However, all of the phase values from juvenile preparations fell within the range of adult values, as can be seen in the histograms in Figure 6*D*. It should also be noted that the differences between phase relationships in juvenile and adult animals are minimal compared with phase shifts that can be induced by neuromodulators (Eisen and Marder, 1984; Weimann et al., 1997).

Phase shifts during cycle-to-cycle period variability within experiments

Mean phase relationships were well preserved across different preparations and relatively well maintained during growth, but does that mean that all the cellular and synaptic parameters that determine phase relationships in the network must be tightly regulated? Theoretical studies have shown that different combinations of maximum conductance values can lead to very similar cell activity (Liu et al., 1998; Goldman et al., 2001; Golowasch et al., 2002; Prinz et al., 2003) and that considerably different combinations of synaptic strengths can lead to similar network activity (Prinz et al., 2004). We wanted to see whether there was any indication of underlying differences between preparations that

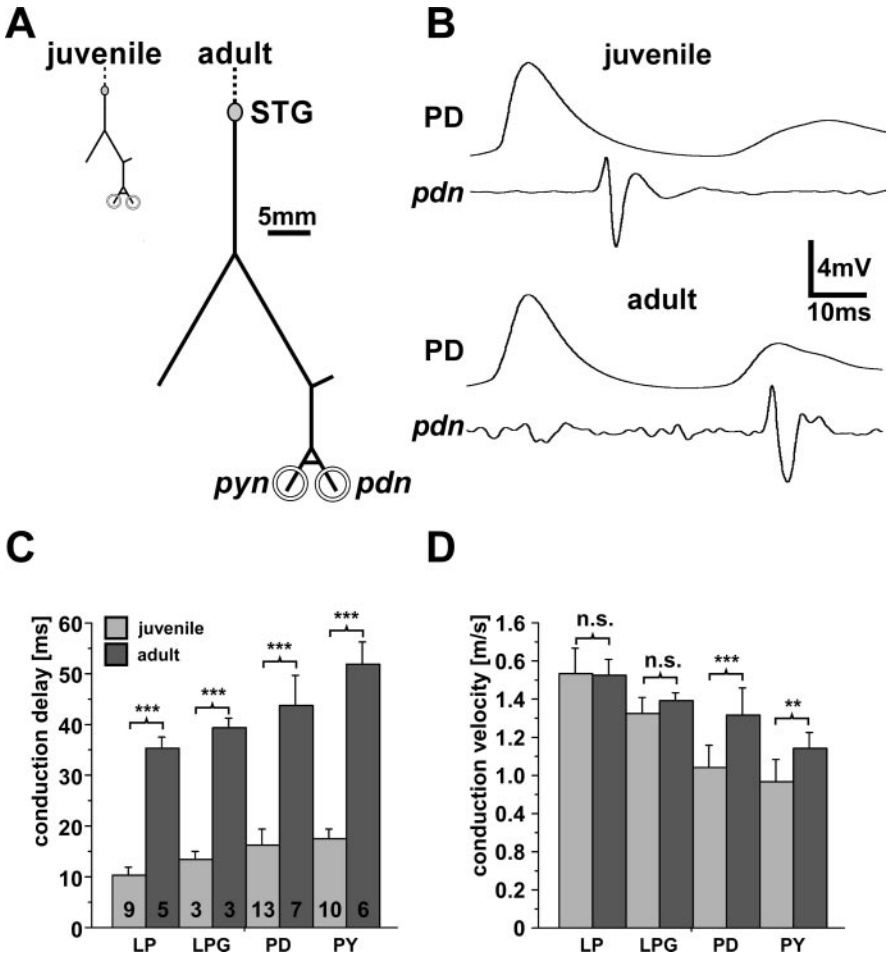

Figure 4. Growth and spike conduction in the peripheral nerves of the stomatogastric nervous system. *A,* Schematic outlines of the peripheral nerves between STG and extracellular recording sites. Relative scaling between different nerves and between juvenile and adult represents means from measurements taken in 10 juveniles and 7 adults. *B,* Averaged traces of intracellular recordings of a PD neuron and extracellular pdn recordings in a juvenile and an adult. The intracellularly recorded peak of the spike was used as a trigger. Note the increase in conduction delay between soma and nerve. *C,* Conduction delays measured from intracellular to extracellular spikes. Indicated are numbers of measurements for the specific cell types recorded in the 10 juvenile and 7 adult STGs (unpaired *t* tests). *D,* Conduction velocities calculated from distance/delay (unpaired *t* tests).

produced similar mean network output. Therefore, we analyzed how consistent the phase values were within experiments. The cycle period in a given preparation did not change systematically within the time window analyzed, but there was sufficient cycle-to-cycle variability to allow us to perform regression analysis for all phase parameters. Figure 7*A* shows phase plots of three preparations with similar mean cycle periods and phase values. Each preparation showed different combinations of slopes for the phases as a function of cycle period. We analyzed all 111 preparations (including the 12 juveniles). Figure 7*B* shows the distributions of slope values for the different phases. Negative slopes were the most common, and correlation analysis showed that the slopes of the different phases were mostly dependent on each other (Bartlett's test of sphericity, $p < 0.001$). However, different slopes and different combinations of slopes were found between different preparations. Correlation analysis showed that the slopes did not depend on the mean cycle period (p values between 0.06 and 0.85; Fisher's r to z tests). Within single preparations, the difference between the longest and shortest cycle period ranged from 76 to 1168 ms (mean: 367 ± 196). The number of cycles analyzed was different from preparation to preparation (51–964; mean: 254 ± 199). Therefore, we tested whether the slopes and the p values found with regression analysis of phase over cycle period were dependent on the cycle period range or the number of cycles analyzed. This was only the case for 2 of 20 measures (for the slope of PD off phase over cycle period, which was dependent on the number of cycles analyzed, and the slope of LP on phase over cycle period, which was dependent on the cycle period range).

Number of spikes and spike frequencies

The phase relationships of pyloric neurons give information about the sequence of bursts and their relative timing, but not about the intensity of motor neuron activity. Muscle contraction also depends on the number of spikes per burst and the spike frequency within a burst. We therefore analyzed spike frequency and the number of spikes in PD and LP neuron bursts. For the PY neurons this was not possible (see Materials and Methods). Figure 8 shows the mean number of spikes per burst (*A*) and the spike frequency within bursts (*B*) over cycle period for the PD and LP neurons. We did not separate the signals from the two PD neurons because there was no discernible difference between the spike patterns, and all pyloric dilator muscles are innervated by both PD neurons. The mean number of spikes per burst was fairly broadly distributed (Fig. 8*A*). The mean number of PD neuron spikes ranged from 13.5 to 49.5 (mean: 30.9 ± 7.1), and the mean number of LP neuron spikes ranged from 3.8 to 21.5 (mean: 11.1 ± 4.0). Regression analysis showed that the number of spikes per burst was not dependent on the mean cycle period (PD: $p = 0.60$; LP: $p = 0.83$). Because the burst durations increased proportionally with the cycle period (Fig. 5), the independence of the number of spikes per burst on cycle period means that the spike frequency within bursts decreased with increasing cycle period (Fig. 8*B*). These negative slopes were significant for the PD neurons and the LP neurons ($p < 0.001$ each). The mean number of spikes per burst in juvenile animals were all in the range of the adults and not statistically different (PD: $p = 0.79$; LP: $p = 0.17$; unpaired t tests).

Discussion

Stability of network output across animals and during growth

Networks of all kinds, and central pattern generating networks in particular, can be described by numerous features of their output patterns. Are any of these features tightly controlled across multiple individuals in the species? Which of these features are most tightly controlled during growth? If there is a set point for some aspect of network function, one way to potentially establish this is to look for features that are tightly regulated, both across individual animals and over years of growth.

Studying network performance during growth provides an interesting tool for understanding regulation of network activity

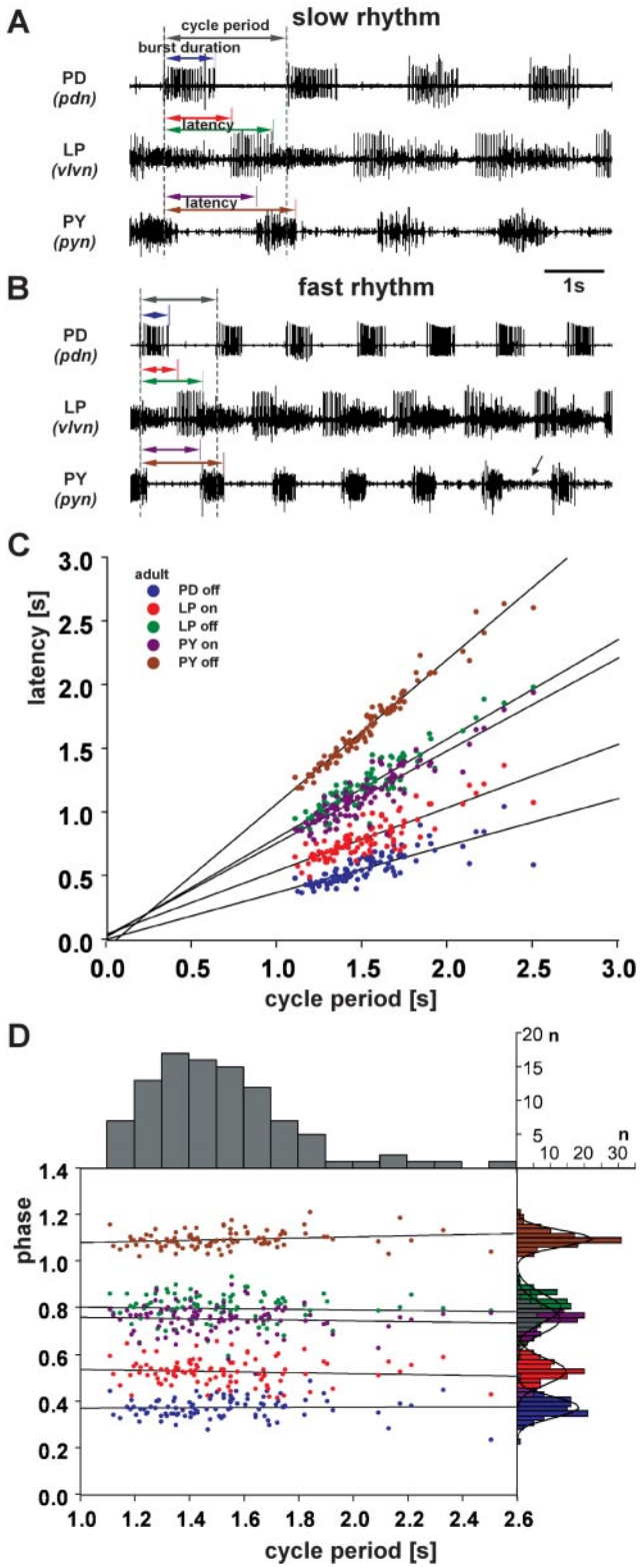

Figure 5. Quantification of the triphasic pyloric rhythm in adult preparations. *A,* Nerve recordings in a relatively slow rhythm. Indicated are the latency measurements taken from the onset of each PD neuron burst. *B,* Nerve recordings in a relatively fast rhythm. The same measurements as in *A* are indicated. The small amplitude signals in the pyn recording (arrow) are the action potentials of the two LPG neurons. *C,* The mean latencies plotted as a function of the mean cycle period from 99 adult preparations. *D,* The mean phase values plotted as a function of the mean cycle period. The histogram at the top of the figure shows the distribution of mean cycle periods from the 99 adult animals. The histograms at the right of the figure show the distributions of the mean phase values. Lines in *B* and *C* are linear regression fits.

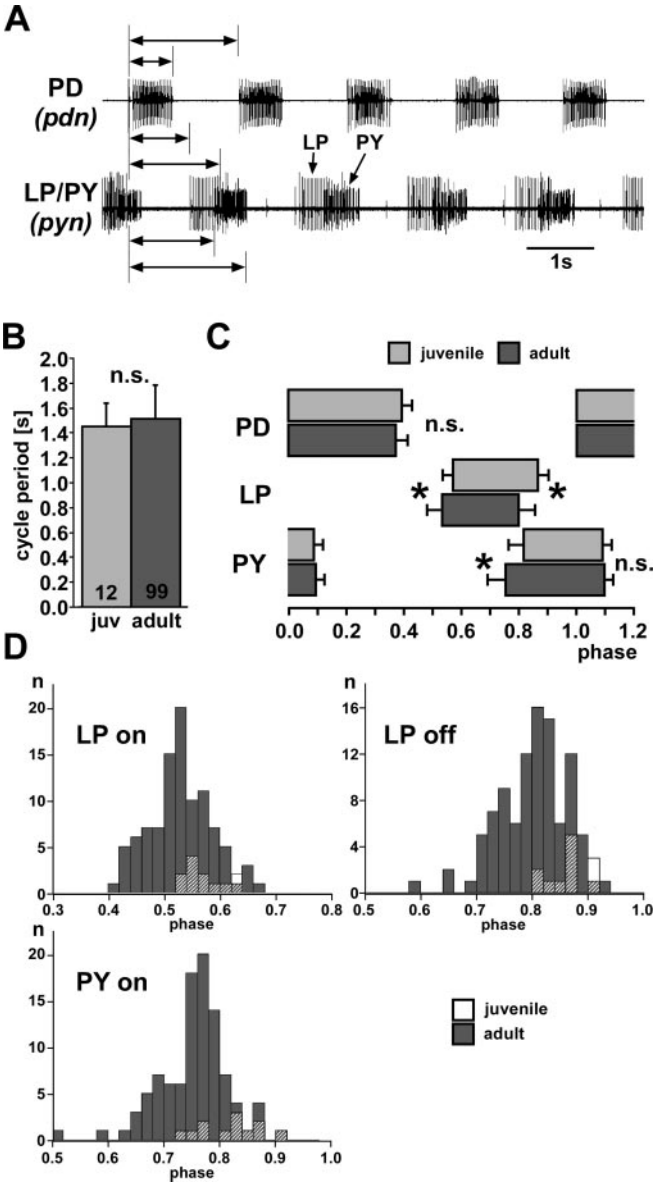

Figure 6. Comparison of the pyloric rhythm in juvenile and adult preparations. *A,* Nerve recordings in a juvenile preparation. Indicated are the same measurements as in Figure 5. *B,* Comparison of the mean cycle periods in 12 juvenile and 99 adult preparations. Unpaired *t* test. *C,* Plot of the mean phase relationships in juvenile and adult preparations. PD off: $p = 0.19$; LP on: $p < 0.05$; LP off: $p < 0.001$; PY on: $p < 0.001$; PY off: $p = 0.78$ (unpaired *t* tests). *D,* Distributions of the phase values that were significantly different in juvenile and adult preparations, as indicated in *C*. Note that all juvenile values lie within the ranges of adult preparations (bin size: 0.02). Overlap of juvenile and adult values is indicated by hatched pattern.

because the increase in neuron size is potentially a challenging problem. Neuronal activity and function are determined by electrotonic structure, receptor and channel distribution and densities, and synaptic connectivity. Diameters and lengths of neuronal processes must be increased at appropriate relative rates to preserve electrotonic structure or to change it in a controlled way (Hill et al., 1994; Olsen et al., 1996). Receptor and channel density regulation must be appropriately matched to the increase in membrane surface area, and synaptic function must be altered in accordance with changes in input resistance in the postsynaptic cells (Edwards et al., 1994b). The STG has the same number of neurons in embryos and adults (Casasnovas and Meyrand, 1995), and the characteristic triphasic pattern and the regularity of the

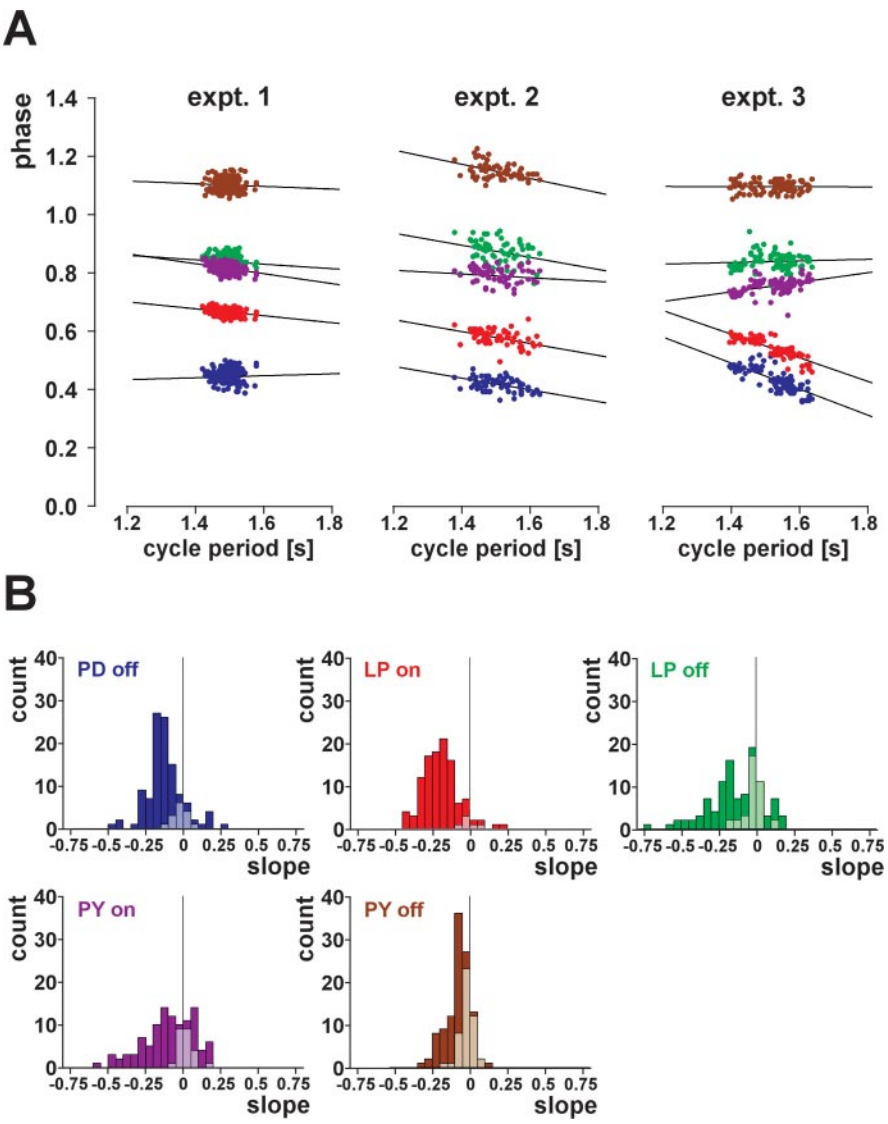

Figure 7. Phase relationships within preparations, quantified from cycle-to-cycle period variability. *A,* Phase relationships in three different preparations with similar mean cycle periods and mean phase values. *B,* Distributions of slope values of phase over cycle period from 99 adult and 12 juvenile preparations (bin size: 0.05). Nonsignificant slopes are shown in light shading.

pyloric rhythm emerge over the course of larval development (Richards et al., 1999). We show here that the STG grows substantially from juvenile to adult animal. Despite changes in ganglion size and shape, and the accompanying change in neuron size, both the characteristic waveforms seen in intracellular recordings and the phase relationships of the pyloric motor pattern in the isolated CNS stay remarkably constant. The constancy of phase relationships is found both between juvenile and adult animals and across animals in adults and in juveniles, although the cycle periods varied considerably. This argues that maintenance of the characteristic triphasic rhythm may be more important than the exact period of the rhythm.

Phase maintenance and phase homeostasis

Phase relationships and period of the pyloric rhythm can be controlled independently (Eisen and Marder, 1984). It is important to note that once the synaptic and intrinsic properties are tuned to yield a specific mean phase value, this phase may be independent of the mean cycle period in a given preparation. The pyloric rhythm in the spiny lobster maintains relatively constant phase relationships when the cycle period is altered by injecting current into the pacemaker neurons (Hooper, 1997a,b). This mechanism is rapid and is observed within a few cycles after the period is altered. How does this phase maintenance relate to the constancy of mean phase values during growth and across different animals that we describe here? For follower neurons in the pyloric circuit (neurons that burst in rebound from synaptic inhibition), phase maintenance of the onset of the burst has been attributed to a combination of synaptic depression and the dynamics of intrinsic conductances (Bose et al., 2004; Greenberg and Manor, 2005). Depressing inhibitory synapses in oscillatory systems promote phase maintenance because their strength increases with cycle period (Manor et al., 2003; Nadim et al., 2003), and A-type potassium currents do so because they will delay rebound from inhibition more at longer cycle periods when the burst duration of the presynaptic neuron is increased (Hooper, 1998). These mechanisms do not provide an explanation for why the phase values are so similar across different preparations, but any long-term regulation of intrinsic and synaptic conductances must result in solutions that can maintain phase when the cycle period is modified on a shorter time scale.

Does constant central pattern generation mean constant motor output?

Some parts of the nervous system require alterations to respond to changing behavioral context or changing body size (Edwards et al., 1994a,b). In other systems, such as feeding or respiration, it may be important that motor output remains constant during growth. The constancy of phase relationships of the pyloric rhythm we show here was measured from isolated preparations of the stomatogastric nervous system. Whether constancy of centrally generated activity patterns implies constant motor output is a different matter. Muscle properties, biomechanics, and sensory feedback may all be different between juvenile and adult animals, and may even be different between different individuals of the same size. For example, the electrical response to bursting input changes in a muscle innervated by the LP neuron during the postmetamorphic growth of the lobster stomach, although the activity pattern of the LP neuron stays primarily unchanged (Pulver et al., 2005). It is therefore possible that central regulatory mechanisms act throughout the postmetamorphic life span to ensure constant network performance both during growth and across different individuals, whereas changes that are adaptive for peripheral motor performance are made at the level of the neuromuscular junction or the muscle itself. Peripheral plasticity may also be important because spike numbers and spike frequencies are not well preserved between animals (Fig. 8). Contraction amplitude is determined by spike frequency in some muscles and by spike number in others (Morris and Hooper, 1997). In con-

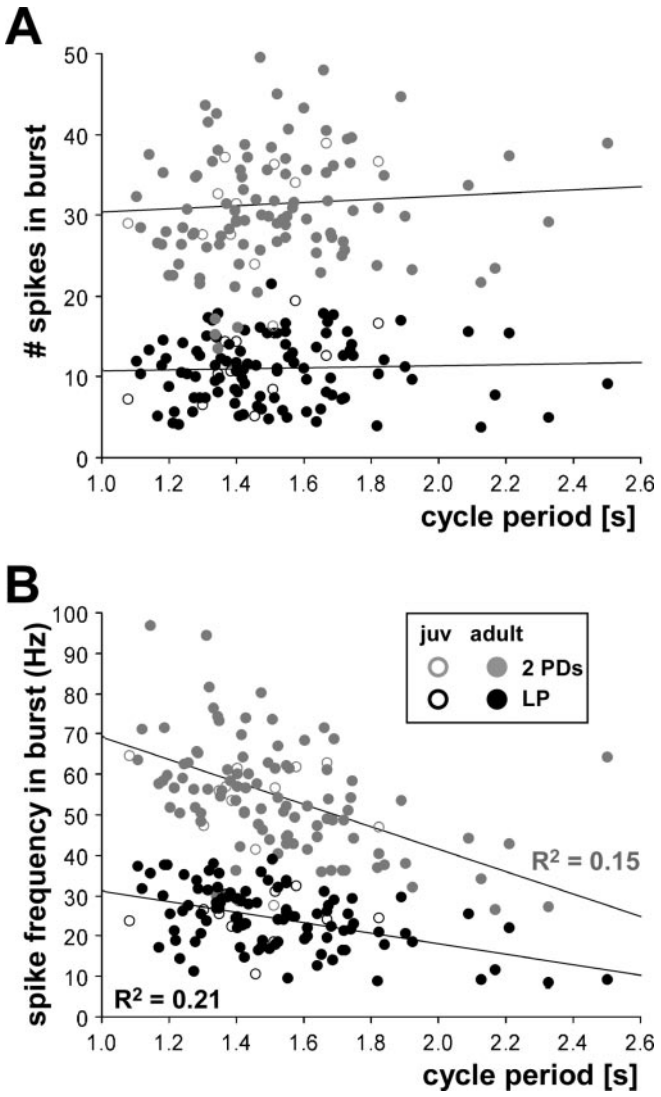

Figure 8. Mean number of spikes per burst and mean spike frequency within bursts from 99 adult and 12 juvenile preparations.

trast, spike-mediated transmission is not necessary for the expression of central pyloric rhythmicity (Raper, 1979), and it is not clear what role it plays (Ayali et al., 1998). Potentially, regulation of spiking may therefore also be independent of the regulatory mechanisms that effect the temporal structure of bursting activity. This is interesting because the overall number of spikes has been used as a measure of mean activity in many systems and has been implicated as the key set-point for activity-dependent homeostatic regulation (Miller, 1996; Turrigiano and Nelson, 2004).

Stability of network output with different network configurations

The consistency of mean phase relationships across animals and during growth could arise from strong regulation toward tightly constrained values of intrinsic conductances and synapse strengths. However, it is doubtful that there is a unique parameter combination that yields "typical" pyloric network activity. A recent modeling study has shown that networks with the same underlying architecture but different combinations of intrinsic conductances and synaptic strengths can produce almost identical activity (Prinz et al., 2004). We show here that the way phase relationships change with cycle period within a given preparation can be different between preparations (Fig. 7), although their mean phase relationships are very similar. The total change in phase values within a given preparation between the slowest and the fastest cycle analyzed was small and may well be functionally insignificant for motor output. However, the different correlations of phase values and cycle period may indicate that different animals have found different combinations of membrane and synaptic currents that give rise to very similar motor patterns. There is experimental evidence that stability of pyloric neuron activity results from activity-dependent homeostatic regulation, both at the level of single neurons (Turrigiano et al., 1994), and on the network level (Thoby-Brisson and Simmers, 1998, 2000; Golowasch et al., 1999b; Luther et al., 2003). Previous theoretical work has shown that simple homeostatic rules in which Ca^{2+} concentrations are used to track activity patterns can regulate both intrinsic properties and synaptic strengths (LeMasson et al., 1993; Liu et al., 1998; Golowasch et al., 1999b; Soto-Trevino et al., 2001).

Could absolute phase values be set-points or targets for regulation? It is possible that the synaptic architecture of the pyloric network "automatically" results in appropriate phase regulation as a consequence of the coordinated tuning of synaptic and intrinsic properties of all the neurons and synapses in the pyloric circuit. Otherwise, we will have to understand how phase itself can be monitored and controlled.

References

Aizenman CD, Akerman CJ, Jensen KR, Cline HT (2003) Visually driven regulation of intrinsic neuronal excitability improves stimulus detection in vivo. Neuron 39:831–842.

Ayali A, Johnson BR, Harris-Warrick RM (1998) Dopamine modulates graded and spike-evoked synaptic inhibition independently at single synapses in pyloric network of lobster. J Neurophysiol 79:2063–2069.

Bose A, Manor Y, Nadim F (2004) The activity phase of postsynaptic neurons in a simplified rhythmic network. J Comput Neurosci 17:245–261.

Bucher D, Scholz M, Stetter M, Obermayer K, Pflüger H (2000) Correction methods for three-dimensional reconstructions from confocal images. I. Tissue shrinking and axial scaling. J Neurosci Methods 100:135–143.

Casasnovas B, Meyrand P (1995) Functional differentiation of adult neural circuits from a single embryonic network. J Neurosci 15:5703–5718.

Davis GW, Bezprozvanny I (2001) Maintaining the stability of neural function: a homeostatic hypothesis. Annu Rev Physiol 63:847–869.

Davis GW, Goodman CS (1998) Genetic analysis of synaptic development and plasticity: homeostatic regulation of synaptic efficacy. Curr Opin Neurobiol 8:149–156.

Desai NS, Rutherford LC, Turrigiano GG (1999) Plasticity in the intrinsic excitability of cortical pyramidal neurons. Nat Neurosci 2:515–520.

Edwards DH, Fricke RA, Barnett LD, Yeh SR, Leise EM (1994a) The onset of response habituation during the growth of the lateral giant neuron of crayfish. J Neurophysiol 72:890–898.

Edwards DH, Yeh SR, Barnett LD, Nagappan PR (1994b) Changes in synaptic integration during the growth of the lateral giant neuron of crayfish. J Neurophysiol 72:899–908.

Eisen JS, Marder E (1984) A mechanism for production of phase shifts in a pattern generator. J Neurophysiol 51:1375–1393.

Factor JR (1995) Biology of the lobster, *Homarus americanus.* San Diego: Academic.

Goldman MS, Golowasch J, Marder E, Abbott LF (2001) Global structure, robustness, and modulation of neuronal models. J Neurosci 21:5229–5238.

Golowasch J, Marder E (1992) Ionic currents of the lateral pyloric neuron of the stomatogastric ganglion of the crab. J Neurophysiol 67:318–331.

Golowasch J, Abbott LF, Marder E (1999a) Activity-dependent regulation of potassium currents in an identified neuron of the stomatogastric ganglion of the crab *Cancer borealis.* J Neurosci 19:RC33(1–5).

Golowasch J, Casey M, Abbott LF, Marder E (1999b) Network stability from activity-dependent regulation of neuronal conductances. Neural Comput 11:1079–1096.

Golowasch J, Goldman MS, Abbott LF, Marder E (2002) Failure of averaging in the construction of a conductance-based neuron model. J Neurophysiol 87:1129–1131.

Greenberg I, Manor Y (2005) Synaptic depression in conjunction with A-current channels promote phase constancy in a rhythmic network. J Neurophysiol, in press.

Harris-Warrick R, Marder E, Selverston A, Moulins M (1992) Dynamic biological networks: the stomatogastric nervous system. Cambridge, MA: MIT.

Hill AA, Edwards DH, Murphey RK (1994) The effect of neuronal growth on synaptic integration. J Comput Neurosci 1:239–254.

Hochner B, Spira ME (1987) Preservation of motoneuron electrotonic characteristics during postembryonic growth. J Neurosci 7:261–270.

Hooper SL (1997a) The pyloric pattern of the lobster (*Panulirus interruptus*) stomatogastric ganglion comprises two phase-maintaining subsets. J Comput Neurosci 4:207–219.

Hooper SL (1997b) Phase maintenance in the pyloric pattern of the lobster (*Panulirus interruptus*) stomatogastric ganglion. J Comput Neurosci 4:191–205.

Hooper SL (1998) Transduction of temporal patterns by single neurons. Nat Neurosci 1:720–726.

Kilman VL, Marder E (1996) Ultrastructure of the stomatogastric ganglion neuropil of the crab, *Cancer borealis.* J Comp Neurol 374:362–375.

LeMasson G, Marder E, Abbott LF (1993) Activity-dependent regulation of conductances in model neurons. Science 259:1915–1917.

Liu Z, Golowasch J, Marder E, Abbott LF (1998) A model neuron with activity-dependent conductances regulated by multiple calcium sensors. J Neurosci 18:2309–2320.

Luther JA, Robie AA, Yarotsky J, Reina C, Marder E, Golowasch J (2003) Episodic bouts of activity accompany recovery of rhythmic output by a neuromodulator- and activity-deprived adult neural network. J Neurophysiol 90:2720–2730.

MacLean JN, Zhang Y, Johnson BR, Harris-Warrick RM (2003) Activity-independent homeostasis in rhythmically active neurons. Neuron 37:109–120.

Manor Y, Bose A, Booth V, Nadim F (2003) Contribution of synaptic depression to phase maintenance in a model rhythmic network. J Neurophysiol 90:3513–3528.

Marder E, Prinz AA (2002) Modeling stability in neuron and network function: the role of activity in homeostasis. Bioessays 24:1145–1154.

Maynard DM, Dando MR (1974) The structure of the stomatogastric neuromuscular system in *Callinectes sapidus, Homarus americanus* and *Panulirus argus* (Decapoda Crustacea). Philos Trans R Soc Lond B Biol Sci 268:161–220.

Miller KD (1996) Synaptic economics: competition and cooperation in synaptic plasticity. Neuron 17:371–374.

Morris LG, Hooper SL (1997) Muscle response to changing neuronal input in the lobster (*Panulirus interruptus*) stomatogastric system: spike number- versus spike frequency-dependent domains. J Neurosci 17:5956–5971.

Nadim F, Booth V, Bose A, Manor Y (2003) Short-term synaptic dynamics promote phase maintenance in multiphasic rhythms. Neurocomputing 52- 54:79–87.

Olsen O, Nadim F, Hill AA, Edwards DH (1996) Uniform growth and neuronal integration. J Neurophysiol 76:1850–1857.

Prinz AA, Billimoria CP, Marder E (2003) Alternative to hand-tuning conductance-based models: construction and analysis of databases of model neurons. J Neurophysiol 90:3998–4015.

Prinz AA, Bucher D, Marder E (2004) Similar network activity from disparate circuit parameters. Nat Neurosci 7:1345–1352.

Pulver SR, Bucher D, Simon DJ, Marder E (2005) Constant amplitude of postsynaptic responses for single presynaptic action potentials but not bursting input during growth of an identified neuromuscular junction in the lobster, *Homarus americanus.* J Neurobiol 62:47–61.

Raper JA (1979) Nonimpulse-mediated synaptic transmission during the generation of a cyclic motor program. Science 205:304–306.

Richards KS, Miller WL, Marder E (1999) Maturation of lobster stomatogastric ganglion rhythmic activity. J Neurophysiol 82:2006–2009.

Rowell CHF (1989) The taxonomy of invertebrate neurons: a plea for a new field. Trends Neurosci 12:169–174.

Segev I, Rinzel J, Shepherd GM, eds (1995) The theoretical foundation of dendritic function. Selected papers of Wilfried Rall with commentaries. Cambridge, MA: MIT.

Selverston AI, Moulins M (1985) Oscillatory neural networks. Annu Rev Physiol 47:29–48.

Soto-Trevino C, Thoroughman KA, Marder E, Abbott LF (2001) Activity-dependent modification of inhibitory synapses in models of rhythmic neural networks. Nat Neurosci 4:297–303.

Stemmler M, Koch C (1999) How voltage-dependent conductances can adapt to maximize the information encoded by neuronal firing rate. Nat Neurosci 2:521–527.

Thoby-Brisson M, Simmers J (1998) Neuromodulatory inputs maintain expression of a lobster motor pattern-generating network in a modulation-dependent state: evidence from long-term decentralization in vitro. J Neurosci 18:2212–2225.

Thoby-Brisson M, Simmers J (2000) Transition to endogenous bursting after long-term decentralization requires de novo transcription in a critical time window. J Neurophysiol 84:596–599.

Turrigiano GG (1999) Homeostatic plasticity in neuronal networks: the more things change, the more they stay the same. Trends Neurosci 22:221–227.

Turrigiano GG, Nelson SB (2004) Homeostatic plasticity in the developing nervous system. Nat Rev Neurosci 5:97–107.

Turrigiano G, Abbott LF, Marder E (1994) Activity-dependent changes in the intrinsic properties of cultured neurons. Science 264:974–977.

Turrigiano G, LeMasson G, Marder E (1995) Selective regulation of current densities underlies spontaneous changes in the activity of cultured neurons. J Neurosci 15:3640–3652.

Weimann JM, Skiebe P, Heinzel HG, Soto C, Kopell N, Jorge-Rivera JC, Marder E (1997) Modulation of oscillator interactions in the crab stomatogastric ganglion by crustacean cardioactive peptide. J Neurosci 17:1748–1760.

Zhang W, Linden DJ (2003) The other side of the engram: experience-driven changes in neuronal intrinsic excitability. Nat Rev Neurosci 4:885–900.